Research article

NMR IN BIOMEDICINE

Received: 11 October 2011, Revised: 6 January 2012, Accepted: 6 January 2012, Published online in Wiley Online Library: 24 February 2012

(wileyonlinelibrary.com) DOI: 10.1002/nbm.2784

Characterization and mapping of dipolar interactions within macromolecules in tissues using a combination of DQF, MT and UTE MRI

Uzi Eliav[a], Michal Komlosh[b,c], Peter J. Basser[b] and Gil Navon[a]*

This study shows that by combining a double-quantum filtered magnetization transfer (DQF-MT) with an ultra-short TE (UTE) MRI that it is possible to obtain contrast between tissue compartments based on the following characteristics: (a) the residual dipolar coupling interaction within the biomacromolecules, which depends on their structure, (b) residual dipolar interactions within water molecules, and (c) the magnetization exchange rate between biomacromolecules and water. The technique is demonstrated in rat-tail specimens, where the collagenous tissue such as tendons and the annulus pulposus of the disc are highlighted in these images, and their macromolecular properties along with those of bones and muscles can be characterized. DQF-MT UTE MRI also holds promise because collagenous tissues that are typically invisible in conventional MRI experiments produce significant signal intensities using this approach. Copyright © 2012 John Wiley & Sons, Ltd.

Keywords: DQF; MT; UTE; dipolar interaction; rat tail; tendons; annulus pulposus; intervertebral disc; short T2

INTRODUCTION

Commonly used clinical MRI methods use water magnetization to obtain anatomical and functional information based on diffusion coefficients and relaxation times. However, these methods provide only limited information about the properties of biomacromolecules (MM) such as collagen that are common in extracellular matrix (ECM) and connective tissues such as cartilage, ligaments and tendons. To obtain better insight into the properties of MM content of the tissue, it is desirable to have methods that probe MM magnetization. Attempts to achieve this goal have used magnetization transfer contrast (MTC). In that method, MM magnetization is fully saturated and the decline in the water signal is monitored. Results depend on the longitudinal relaxation (T_1) of water and its rate of exchange with the MM, and thus provide only limited information about the identity and nature of MMs. It has been argued, however, that by considering the level of B_1 and the frequency offset from the water, that MTC MR might yield a distribution of T_2 values of the MM (1).

Another method to select the subpopulation of MM-associated protons is with double quantum filtering (DQF) MRI (2–6). This approach allows for the selection of the protons to be excited based on the strength of their dipolar interactions and is therefore more sensitive to MM properties, thereby facilitating contrast based on these properties. Since water molecules are highly mobile their intramolecular dipolar interactions largely average out. This characteristic can be used to suppress the water signal and retain only the MM protons whose motions are highly restricted and whose dipolar interactions do not entirely average out. Indeed, spectroscopic studies of MMs such as collagen yielded a spectral width of tens of kHz. Such a large spectral width cannot be detected by MRI, even with methods that use a very short echo time (TE). In previous studies of neuronal systems, this difficulty was solved by using DQF-MT, where the MM transverse magnetization was converted to the longitudinal axis and subsequently to water magnetization by proton exchange (3) whose magnetization could be used for imaging (6). Though this method provides detailed information about MMs in neuronal systems, its application to connective tissues is still restricted by the short water transverse relaxation time (T_2), thereby limiting the use of popular imaging methods such as gradient and spin-echo MRI and requiring large slice thicknesses and low voxel resolutions. These limitations have made the study of MM content and composition difficult. Recently, methods using ultra-short TE (UTE) have enabled imaging of tissues with short T_2 such as tendons. (7–10). As a result, in the present study, DQF-weighted NMR was combined with UTE MRI to obtain images with contrasts that distinguished tissue compartments based on differences in their MM content.

* *Correspondence to: G. Navon, School of Chemistry, Tel Aviv University, Levanon Street, Tel Aviv, 69978, Israel.*
E-mail: navon@post.tau.ac.il

a *U. Eliav, G. Navon*
School of Chemistry, Tel Aviv University, Tel Aviv, Israel

b *M. Komlosh, P. J. Basser*
Section on Tissue Biophysics and Biomimetics (STBB), Eunice Kennedy Shriver National Institute of Child Health and Human Development (NICHD), NIH, Bethesda, MD, USA

c *M. Komlosh*
Center for Neuroregenerative Medicine (CNRM) and the Henry Jackson Foundation (HJF), Bethesda, MD, USA

Abbreviations used: *DQF, double-quantum filter; ECM, extracellular matrix; GE, gradient echo; MM, macromolecules; MT, magnetization transfer; MTC, magnetization transfer contrast; TE, time to echo or echo-time; UTE, ultra-short TE; FID, free induction decay.*

NMR IN BIOMEDICINE

Theoretical background and pulse sequences

Dipolar interaction between nuclei is a function of their distance ($1/r^3$) and orientation of the internuclear vector with respect to the external magnetic field. In well-ordered systems, this interaction leads to a well-resolved spectrum. In systems where the orientations of the internuclear vectors are partially ordered or randomly distributed, the spectral lineshape will vary between a Pake doublet and a Gaussian, respectively. Moreover, dynamic processes such as reorientation and chemical exchange cause reductions in the observed dipolar interaction to an extent that depends on the rate and anisotropy of the motion. For MMs such as collagen in connective tissues for which the motions are slow or anisotropic and where chemical exchange has no effect, dipolar interactions between protons are not significantly reduced (having order parameters in the range 0.3-1.0) and their size is in the tens of kHz. Such a large interaction manifests itself with spin dynamics on a time scale of a few tens of μs. For bound water molecules on the other hand, the intramolecular dipolar interactions are significantly reduced as a result of their fast isotropic or anisotropic reorientational motion, their exchange with the bulk water, and the exchange between binding sites with different average orientations. Furthermore, proton exchange between water molecules causes an additional reduction in the proton-proton intramolecular dipolar interaction (3). The latter process is affected by temperature (3), pH (Eliav, Seo and Navon, unpublished results), and buffer concentration (11). It has been shown that ^{1}H water NMR spectra in ordered systems such as collagen fibres and tendons, where proton exchange among water molecules were suppressed either by cooling or by reducing the amount of free water, resulted in a splitting due to residual dipolar interactions (3,12,13). For water, typical residual dipolar interactions were less than 1 kHz and therefore, the spin dynamics occurred on a time scale of hundreds of μS. When the rate of proton exchange between water molecules was greater than the residual dipolar interaction, coalescence of splitting occurred and the linewidth was given by $1/T_2 = \omega_D^2/\kappa$, where ω_D is the dipolar interaction and κ is the proton exchange rate (3).

Dipolar interaction leads to the formation of high rank tensors such as $I_{x1}I_{z2}$ (1 and 2 indicate the interacting protons) that can be selected by DQF (14). It has further been shown that the intensity of this observed signal might depend on the dipolar interaction ω_D, making it possible to distinguish among compartments by these interactions (3,6). However, the population of immobile or restricted MM-associated protons that can be selected and excited using DQF are not sufficient in themselves to produce a strong MR signal suitable for MRI acquisition due to their large ω_D that causes a fast decay of the MM transverse magnetization. As a result, another step is required to amplify the signal due to the MM-associated protons. This is performed using an MT aproach presented in the DQF-MT pulse sequence described below (Fig. 1). This method enables to study the effects of the residual dipolar interaction in tissues, to gain information about water intramolecular dipolar interaction and MM content, and to obtain a new and measurable contrast by MRI on the basis of this information. In Figure 1, gradient echo (GE) is used as an imaging block. However, in the following, we also show results where 2D ultra short TE (2D-UTE) is used for image formation. For spectroscopic studies, the imaging module was replaced by a single 90° pulse followed by signal acquisition.

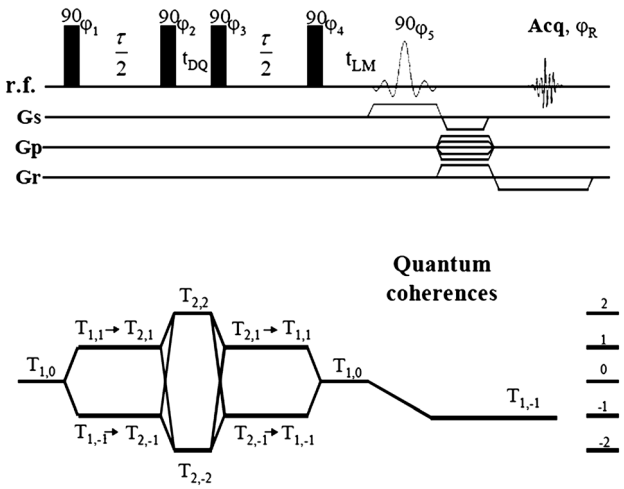

Figure 1. Schematic presentation of the DQF-MT MRI pulse sequence using the gradient-echo imaging modality. The duration of 90° hard pulses was 22 μs. The phase cycling was eight steps given by: $\varphi_1 = \varphi_2 = 0°$ 90° 180° 270°; $\varphi_4 = \varphi_3 = 0°$ 0° 0° 0° 90° 90° 90° 90° ; $\varphi_5 = 0°$; $\varphi_R = 0°$ 180° 0° 180° 180° 0° 180° 0°.

In the DQF-MT pulse sequence, single-rank single-quantum coherences $T_{1,\pm1}$ (given by $\mp I_\pm/\sqrt{2}$) were obtained after the application of the first 90° pulse and evolved during the creation time τ/2 to become second rank tensors $T_{2,\pm1}$, which consist of product operators such as $I_\pm^1 I_z^2$. These were filtered through double quantum coherences $T_{2,\pm2}$ ($I_\pm^1 I_\pm^2/2$) by suitable phase cycling (2–6,14). The filtered tensors reverted to $T_{2,\pm1}$ by application of the third pulse and then evolved during the second τ/2 (reconversion) period into $T_{1,\pm1}$. These tensors were further transformed to $T_{1,0}$ by the fourth pulse and subsequently converted into the observable tensor $T_{1,-1}$ by the last 90° pulse to yield an in-phase spectrum (i.e. similar to a spectrum obtained in a single-pulse free induction decay (FID) experiment) with an intensity proportional to $M_{eq}\mathrm{Sin}^2(\omega_D\tau/2)$. For creation time (τ/2) values that fulfil the condition $\omega_D\ \tau/2 << 1$, the amplitude of the observed signal was proportional to $M_{eq}\omega_D^2$ (M_{eq} is the magnetization at equilibrium, reference 3). This dependence on the interaction and number of protons makes it possible to distinguish between spectra originating from different compartments which, as discussed above, can be distinguished either by the water's intramolecular residual dipolar interaction within the compartment or by the dipolar interaction of its MMs. Similarly in MRI, based on the same differences among the compartments, this pulse sequence yielded a new type of contrast.

When only the longitudinal magnetization of the protons with ω_D typical of the largest dipolar interactions in MM were selected at $t_{LM} = 0$, dipolar interaction induced spin diffusion between these protons and others that were not selected (4) occurred. This process reached a pseudo-equilibrium state typically within 1–2 ms, where the observed spectrum resembled that of the MMs obtained after a single 90° pulse for samples where the water signal did not interfere (e.g. samples where water was replaced by D_2O). Since τ/2 was selected to be compatible with MM dipolar interaction but too short to enable excitation of the water, whose ω_D is much smaller than that of MM at the stage of pseudo-equilibrium, only a small water signal was observed. For t_{LM} periods longer than 1–2 ms, MT between MM

and water occurred. In the following discussion, we redefine the time of pseudo-equilibrium as $t_{LM}=0$. For the case where at pseudo-equilibrium only MM magnetization was retained, the following conditions applied: $m_{zw}(t_{LM}=0)=0$ and $m_{zp}(t_{LM}=0)\neq 0$. In the following discussion, m_{zw} and m_{zp} are the longitudinal magnetizations of water and MMs, respectively, that were obtained after the DQ filter immediately after pseudo-equilibrium was established. As a result, only the transfer of the magnetization m_{zp} ($t_{LM}=0$) to water during the t_{LM} period was observed in the experiment shown in Figure 1. In previous studies of tendons (4,6), it was shown that the transfer mechanism between MM and water is dominated by proton exchange between them. In addition, since the two most visible compartments in the images of rat tail described below consisted of collagen, it can be assumed that proton exchange is the most important transfer process in the rat tail. From a mathematical prospective while conducting phase cycling, the effect of the phases of the RF pulses that preceded the time interval t_{LM} was to multiply $m_{zp}(t_{LM}=0)$ by the phase $e^{i\phi_R}$, where $\phi_R=\pm(\phi_1+\phi_2)\pm(\phi_3+\phi_4))$ (Eq. [2a]) and by $e^{-i\phi_R}$ during acquisition (Eq. [2b]). For a single site, the detected MM magnetization m_{-p} ($m_- = m_x - im_y$) obtained after the last pulse is given by Equation [2a]:

$$m_{-p}=\frac{\sqrt{2}}{2}\left\{m_{zp}(t_{LM}=0)e^{-\frac{t_{LM}}{T_1}}e^{i\phi_R}+m_{eq}^{p}\left(1-e^{-\frac{t_{LM}}{T_1}}\right\}\right. \quad [2a]$$

$$m_{-p}=\frac{\sqrt{2}}{2}\left\{m_{zp}(t_{LM}=0)e^{-\frac{t_{LM}}{T_1}}+e^{-i\phi_R}m_{eq}^{p}\left(1-e^{-\frac{t_{LM}}{T_1}}\right\}\right. \quad [2b]$$

$$m_{-p}=\frac{\sqrt{2}}{2}m_{zp}(t_{LM}=0)e^{-\frac{t_{LM}}{T_1}} \quad [2c]$$

In this expression, there are two contributions to m_{-p}: the first originating from the magnetization immediately after the fourth 90° pulse that is multiplied by the phase $e^{i\phi_R}$ and the second from the magnetization formed during the interval t_{LM} by longitudinal relaxation, which is not multiplied by that phase. During acquisition following the last pulse, both contributions to the signal were multiplied by the phase $e^{-i\phi_R}$ (Eq. [2b]). As a result of the phase cycling on ϕ_R, the second term in Equation [2b], which depends on the longitudinal relaxation and not on the transverse magnetization spin dynamics within the MM, was eliminated (Eq. [2c]).

For exchange between the two sites, it was shown in a previous study (4) that under the initial conditions mentioned above [$(m_{zw}(t_{LM}=0)=0, m_{zp}(t_{LM}=0)\neq 0)$] and the fast exchange limit ($k >> 1/T_1$), where k is the sum of the MT rates from the MM to the water and that of the reverse reaction, the detected magnetizations of water and MM m_{-w} and m_{-p} respectively, are given in Equation [3]:

$$\begin{aligned} m_{-p}&=\frac{\sqrt{2}}{2}m_{zp}(t_{LM}=0)\left(p_p e^{-\frac{t_{LM}}{T_1}}+p_w e^{-kt_{LM}}\right)\\ m_{-w}&=\frac{\sqrt{2}}{2}m_{zp}(t_{LM}=0)p_w\left(e^{-\frac{t_{LM}}{T_1}}-e^{-kt_{LM}}\right)\\ \frac{1}{T_1}&=p_pR_{1p}+p_wR_{1w}\end{aligned} \quad [3]$$

where $m_{zp}(t_{LM}=0)=m_{eq}^{p}\mathrm{Sin}^2(\omega_D^p\tau/2)e^{-\tau/T_2}$, m_{eq}^{p}, ω_D^p and T_2 are the MM equilibrium magnetization, intramolecular dipolar interaction and transverse relaxation, respectively, and $R_{1p}=1/T_{1p}$, $R_{1w}=1/T_{1w}$ with T_{1p}, T_{1w} are the longitudinal relaxation times of MMs and water, respectively. The fractions of the protons residing on the MMs and in water are given by p_p and p_w, respectively. From Equation [3], it is clear that during MT that the water signal is given by a difference of two exponentials: one that characterizes the buildup due to an exchange process and the other that describes the decay due to longitudinal relaxation (with rate given by $1/T_1$). Experimentally, this was confirmed in previous studies of MMs and water signals (4,6) and in the current study for MMs (Figs. 3, 4) where it is shown that for long t_{LM}, the signal decayed off. More generally, longitudinal relaxation was observed as a decay process when prior to its monitoring phase, cycling that selected passage through the transverse plan was implemented.

In addition to the changes in the water signal, MM magnetization was decaying bi-exponentially. It is worth noting that for $t_{LM}/T_1 << 1$, Equation [3] shows that the sum of the water and MM magnetizations equal $m_{zp}(t_{LM}=0)$. However, for widely used conditions in studies of tissues, $t_{LM} > 1/k$, $t_{LM} << T_1$ and $p_w \approx 1$, the water signal, is proportional to $m_{zp}(t_{LM}=0)$. This result is summarized in Equation [4]:

$$m_{zw}\ \ t_{LM}\mathrm{at}\ \max_{\mathrm{intensity}}\ =m_{zp}(t_{LM}=0) \quad [4]$$

It is worth noting that under the conditions that make Equation [4] valid, the MT between the MMs and the water had reached chemical equilibrium but the effect of longitudinal relaxation was negligible. For the case of selective excitation of the water, expressions similar to those in Equation [3] were obtained by interchanging the subscripts *p* and *w*.

From the above discussion, it follows that the DQF-MT sequence enables the experimenter by judicious choice of τ and t_{LM} to obtain MRI contrast that reflects differences among various compartments based on: (a) the number of the MM protons, (b) MM dipolar interactions, and (c) exchange rates between MMs and water. In the following sections, we demonstrate for several systems the effect of the tissue properties such as order, MM content, and exchange rate on the images obtained with the pulse sequences DQF-MT (Fig. 1).

EXPERIMENTAL

Spectroscopic NMR and MRI experiments were conducted on a 14.1 T Bruker micro-imager (Brucker Biospin, Germany). For imaging studies, the pulse sequence shown in Figure 1 was used either with GE as shown or with a commercially available 2D ultra-short TE pulse sequence (Bruker's 2DUTE program running within Bruker's operating system Paravision version 5.1) (7–10). For spectroscopic purposes, the MRI module was replaced by a single 90° pulse. The hard 90° pulses shown in Figure 1 were 22 μs. The ranges of values examined for τ and t_{LM} were 5-400μs and 0.001–600 ms, respectively. The UTE method was optimized by comparison with gradient echo (GE) images of a porcine spinal cord that had a T_2 relaxation time longer than the TE used in the GE method (3.1 ms). The combined DQF-MT and UTE experiments were performed on the part of the rat tail that is the closest to the animal's body. It was skinned, immersed in perfluoropolyether (Fomblin® LC/8, Solvay Solexis, Italy), and then placed in a 10-mm Shigemi tube (Shigemi, Japan) to reduce susceptibility artefacts. The samples were aligned with their cylindrical symmetry axis parallel to the magnetic field.

NMR IN BIOMEDICINE

RESULTS AND DISCUSSION

NMR Spectroscopy

In Figure 2, spectra of rat tail obtained by DQF-MT are shown as a function of the creation/reconversion periods; $\tau/2$ at very short (10 μs) t_{LM}. Two types of spectra are evident. For $\tau \leq 70$ μs, a very broad component with a line width > 10 kHz was observed (Fig. 2a), while for longer time scales, a single peak of ~ 900 Hz line width emerged (Fig. 2b), reaching a maximum intensity for $\tau/2$ in the range of 300-400 μs. The width of this peak was maintained over a large range of creation/reconversion times (25-600 μs) and thus can be attributed to a single species.

By setting $\tau/2$ in the range of 5-80 μs (typical for MM transverse magnetization, 4,6) and examining the dependence on t_{LM}, we obtained the spectra shown in Figure 3. Two major physical processes are noted in Figure 3 (See also ref. 4). On a time scale, shorter than 0.8 ms fast-spin diffusion within the MMs caused the spectrum to converge to an unchanging shape for $t_{LM} > 0.8$ ms (Fig. 3a) but its amplitude decayed off with a concomitant increase in a narrow peak that was attributed to water. This assignment was based on previous spectroscopic studies on tendon, where a similar peak of ~ 900 Hz width was attributed to the water, since it disappeared upon replacement of the H_2O in the sample with D_2O (4). This peak reached its maximum intensity at $t_{LM} = 100$ ms. The intensity of the MMs decayed by a factor of ~ 4 for $t_{LM} = 12$ ms and by at least 8 for $t_{LM} = 100$ ms. Since no narrow peak was observed at short t_{LM}, it is clear that the water peak seen at $t_{LM} = 100$ ms originated solely from magnetization transfer from the MMs. It is evident from Figure 3b that during the exchange process, two peaks of different line widths (both < 1 kHz) were formed. One of the peaks had a width of 900 Hz while the other had a line width of 70 Hz ($T_2 \sim 4.5$ ms). The 900 Hz line resembled the water signal in tendon ($T_2 \sim 350$ μs). An estimate of 1–1.5 s for T_1 of the above two components was obtained from the decay of the signals as shown in Figures 3b and 4b. The narrower of the two peaks might be identified with the water signal in the annulus fibrosus, since its T_2 was reported to be 19 ms (15), which is compatible with the width reported in the current study, taking into account possible inhomogeneity and susceptibility effects. Contribution to this peak from the nucleus pulposus was expected to be limited since it contained small amounts of collagen, while proteoglycans represent the major fraction of the nucleus' MM content. These proteoglycans did not contribute to the DQF-MT since their high mobility reduced their residual dipolar interaction. This assignment is further supported by the imaging results described in the next section.

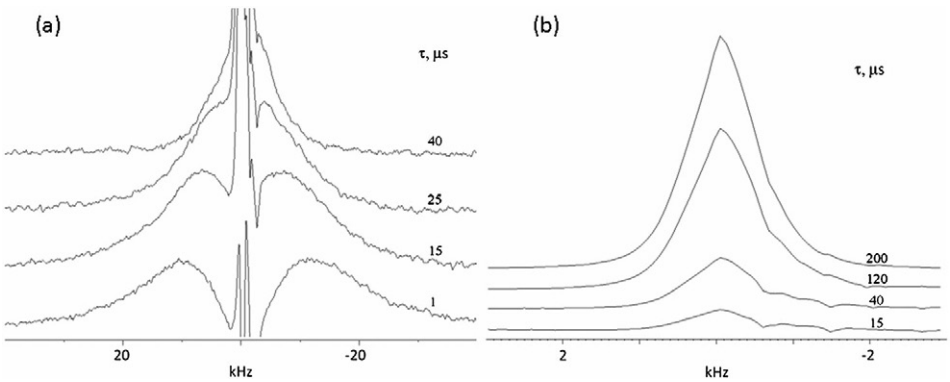

Figure 2. Dependence of ^{1}H rat tail spectrum on creation/reconversion times $\tau/2$ using the pulse sequence shown in Figure 1 (DQF-MT) where the imaging modality was replaced by a single 90° pulse. The shown spectra are drawn on two spectral ranges: (a) the tens of kHz range suitable to display the MM spectra; (b) the few kHz range suitable to display the water molecules spectra. $t_{LM} = 1.5$ μs.

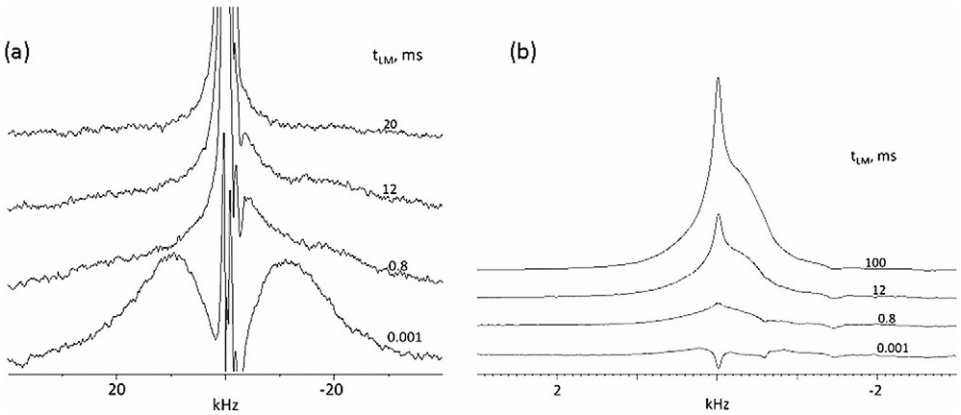

Figure 3. Dependence of ^{1}H rat tail spectrum on exchange time t_{LM} using the pulse sequence shown in Figure 1 (DQF-MT) where the imaging modality was replaced by a single 90° pulse. The shown spectra are drawn on two spectral ranges: (a) the tens of kHz range suitable to display the MM spectra; (b) the few kHz range suitable to display the water molecules spectra. The creation/reconversion time $\tau/2$ was 10 μs.

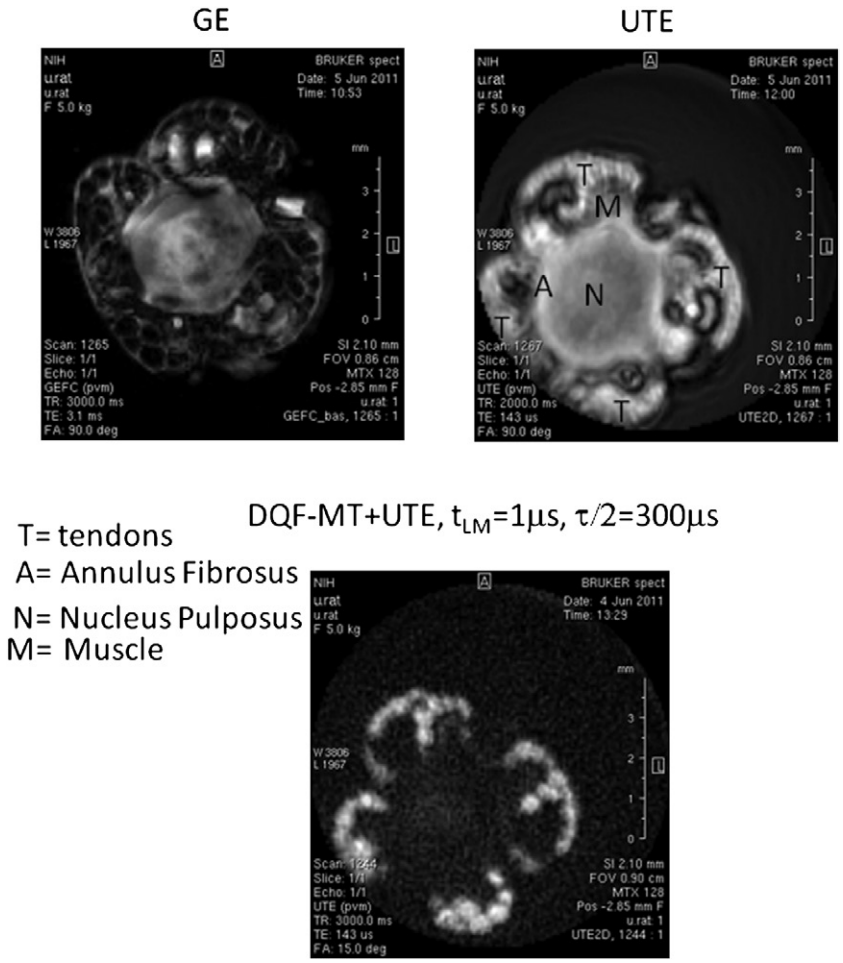

Figure 4. Images of axial slice of rat tail disc obtained using gradient echo, UTE and DQF-MT combined with UTE. Combining DQF-MT with gradient echo gave no image for TE of 2.86 ms since the tendon signal had already decayed away. For UTE-related methods: TE = 0.14 ms, matrix size = 256 x 256, slice thickness = 1.86 mm. The selective RF pulse duration was 0.1 ms. Dead time after echo slice was 2 μ s. TR = 2 s, number of averages = 8. The creation/reconversion time τ/2 in the DQF-MT-weighted UTE image was 300 μ s. t_{LM} = 1.5 μ s.

MRI

In Figure 4, images of an axial slice through a disc of the most superior portion of the rat tail were obtained by gradient echo (GE) and UTE and the latter method weighted by DQF-MT. In the GE images with TE of 2.86 ms, the tendons are absent. Only the annulus fibrosus and the nucleus pulposus are visible as well as the thin layers of para-, epi- and peri-tendineum (16) surrounding the tendons. The UTE method makes the tendons appear with positive contrast, reflecting the fact that weighting by T_2 is less important than in GE. Since the duration of the gradients used for the imaging were 2 ms (both for GE and UTE), which is too long to image macromolecules such as collagen that dephase on a time scale shorter than 80μ s, the contrast obtained by UTE was mostly due to the proton density of the water molecules. However, the short TE diminished the contrast between the annulus fibrosus and nucleus pulposus as well as between the tendons and their surrounding tissue, i.e. the SNR of the tendons, annulus fibrosus and muscles were similar (Fig. 4). This shortcoming was addressed by combining UTE with DQF-MT (bottom of Fig. 4) with the creation/reconversion times set to 300 μ s. In this image, only the tendons are visible, thus confirming that the peak of 900 Hz width (Fig. 1) was due to residual dipolar interactions of bound water in tendons. It is worth noting that the para-tendineum (16) in close proximity to the tendons was absent from the DQF-MT weighted UTE MRI, although present in the UTE images. As explained in the theoretical background section, combining DQF-MT and UTE can yield images with contrasts that reflect differences in MM characteristics. For rat tail, it was expected to distinguish between various types of collagen that constitute the tendons and the annulus fibrosus, e.g. Type I and Type II collagens. In Figure 5, we show UTE MRIs weighted by a DQF-MT sequence. As can be observed, only two parts of the rat tail are clearly visible: the tendons and the annulus, while there is some contribution from muscles in the images obtained for τ/2 = 10 μ s. For this value of τ/2 and t_{LM} in the range of 50–600 ms, the ratio of the SNR of tendon and annulus fibrosus was 1.6, i.e. very different from the equal value observed in the UTE images. Furthermore, since spectroscopic measurements showed that for τ/2 = 10 μ s, the contribution of intramolecular dipolar interaction of the water was negligible and the contrast in the UTE images very small, we attribute the contrast between the tendon and annulus to differences in collagen type or content. This conclusion is consistent with the known difference in the collagen composition of tendons and annulus (17). Tendons mostly consist of collagen type I, while

NMR IN BIOMEDICINE

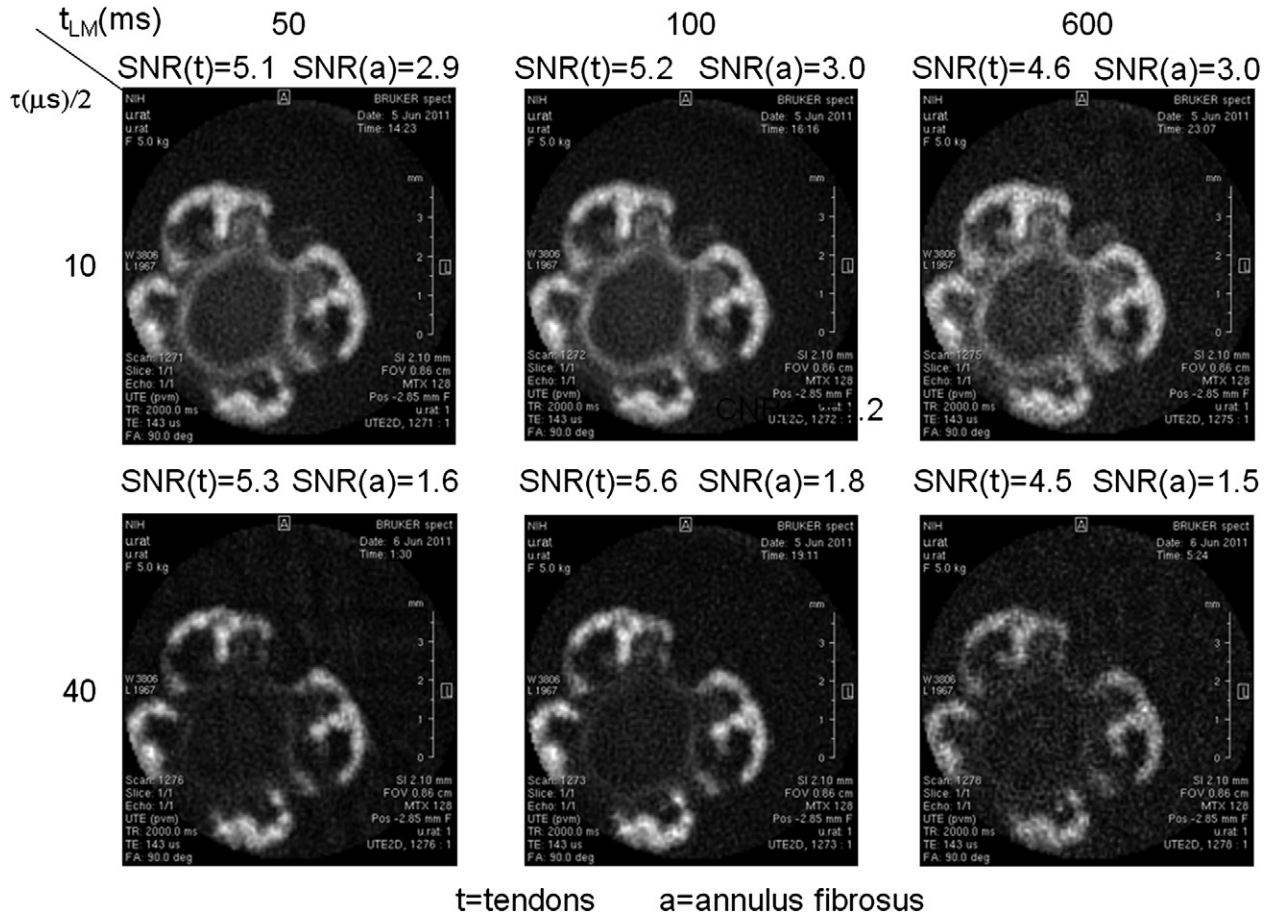

Figure 5. Images of axial slice of rat tail through disc that was obtained using DQF-MT combined with UTE are shown as a function of creation/reconversion time τ/2 and exchange time t_{LM}. Matrix size = 256 x 256, slice thickness = 2.1 mm. The selective RF pulse duration was 0.1 ms. Dead time after echo slice was 2 μs. TR = 2 s, number of averages = 8. The SNR of the tendons (t) was calculated as an average of the SNRs of all tendons and similarly, the SNR for annulus (a) was calculated by taking into account all the area of this tissue.

the annulus contains both types I and II collagen (18) with the former being abundant in the outer part of the annulus and the latter in the inner part closer to the nucleus pulposus. Examining the dependence of the images on the creation/reconversion periods τ/2, we observed that the signals from the tendons, annulus and muscles decayed off on the time scale of tens of μs. However, the extent of their intensity fall-off resulting from increasing τ/2 from 10 to 40 μs was different, namely by factors of 1.0, 2.0, and 1.5 for tendons, annulus fibrosus, and muscles, respectively. Therefore, we concluded that on a creation/reconversion time scale of tens of μs, it was the MM spin dynamics that dominated the MRI signal. This conclusion is further supported by the fast decay of the DQ coherence during the time interval t_{DQ} occurring on a time scale shorter than $t_{DQ} = 80$ μs. This fast decay can be the sole result of spin systems where two dipolar interactions are involved: for instance, dipolar interaction between protons in one CH_2 group and protons in another CH_2 group or in CH or CH_3 groups. It is worth noting that the lack of decay of the tendon's signal could be the result of a combined effect of a decay of the MM magnetization compensated by a signal buildup due to the intramolecular dipolar interaction of the water. This buildup could be more significant for the tendon relative to other tissues in the rat tail based on the larger residual interaction of water in the tendon. From spectroscopic studies, the contribution from the water residual intramolecular interaction at $\tau/2 = 40$ μs can be as large as 40%, as was estimated in the following manner: upon changing τ/2 from 10 μs to 40 μs with $t_{LM} = 1$ μs, the water signal increased by a factor of 3.5 while MM intensity decreased by a factor of 3. Since the amount of magnetization that can be transferred to water is proportional to MM magnetization, a simple calculation yields that at least 40% of the water signal in tendon acquired with $\tau/2 = 40$ μs and $100\,\text{ms} < t_{LM} < 300$ ms can be attributed to a buildup due to water residual intramolecular dipolar interaction. Since the water residual intramolecular interaction in the annulus and muscle was small, the water DQF-MT signal buildup at $\tau/2 = 40$ μs due to this interaction can be neglected. As a result, the difference in the decay of the signals as a function of τ/2 between these two tissues was solely due to differences in their MM structures.

For short creation times, the dependence on the exchange period t_{LM} showed a maximum at 200 ms and was similar for tendons and the annulus. This similarity might suggest that the exchange with water proceeded through similar functional groups present on the collagen backbone, i.e. labile protons of hydroxyproline or hydroxylysine. Further demonstration of the capability of DQF-MT when combined with UTE to distinguish between tissues based on their MM differences is shown in Figure 6, where an axial slice through a vertebrae located in the middle between two discs is shown. As in the case

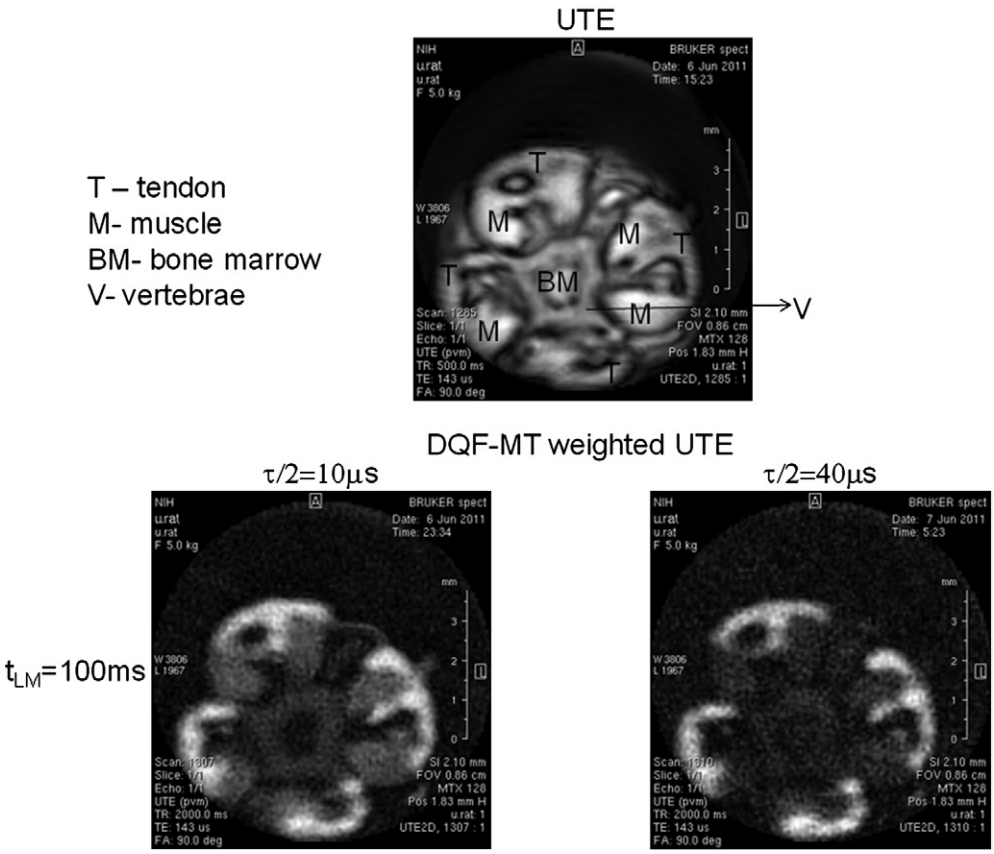

Figure 6. Images of axial slices in a middle point between two disc of rat tail obtained either by using UTE (upper image) or by DQF-MT combined with UTE (bottom line). The latter images are shown as a function of creation/reconversion time (τ/2) for exchange time that yields maximum intensity (t_{LM} = 100 ms). Matrix size = 256 x 256, slice thickness = 2.1 mm. The selective RF pulse duration was 0.1 ms. Dead time after echo slice was 2 μs. TR = 2 s, number of averages = 8.

of the disc, the contrast between the various tissues in the DQF-MT-weighted UTE images were very different from the one obtained by UTE. For the UTE experiment, SNR's of 6.8, 8.8 and 7.2 were obtained for the tendon, muscle and bone, respectively (Fig. 6). The addition of DQF-MT weighting with $\tau/2 = 10\,\mu s$ eliminated the contribution from the bone marrow and set the SNRs (for eight scans) of the tendons, muscles and vertebrae to 8.7, 4.6 and 2.9, respectively. Using the same arguments as in the discussion of the results obtained with $\tau/2 = 10\,\mu s$ for the disc, we might conclude that differences between the various tissues reflected differences in MM contents and structure. Furthermore, examining the dependence of the images on the creation/reconversion periods, τ/2 showed that tendons, muscles and vertebrae decayed on a time scale of tens of μs, indicating that the decay was dominated by MM magnetization. However, the extent of the intensity decay as a result of increasing τ/2 from 10 to 40 μs was different: 1.3, 1.9 and 1.5 for tendons, muscles and vertebrae respectively, reflecting differences in the MM structure.

CONCLUSIONS

In the present work, we demonstrated that combining a DQF-MT "filter" with UTE MRI produced image contrast that was based on the residual dipolar interactions, either within the water molecules or the macromolecules. It was further demonstrated that this new type of contrast makes it possible to distinguish among various compartments within the rat tail on the basis of differences in their macromolecular properties. The prospect of possibly being able to distinguish among different types of collagen could have far-reaching consequences in diagnostic applications, particularly in orthopaedics where there is a dearth of successful MR methods for imaging ECM, intervertebral discs, cartilage, bone, tendons and ligaments.

Acknowledgements

GN and UE were supported by grants from the US–Israel Binational Science Foundation no. 2007157, the European PF7 program ENCITE and the Israel Ministry of Science and Technology No. 3–6446. PJB was supported by the Intramural Research Program of the Eunice Kennedy Shriver National Institute of Child Health and Human Development, NIH. MK was supported by the Center for Neuroregenerative Medicine (CNRM) and the Henry Jackson Foundation (HJF). We gratefully acknowledge Daryl DesPres and Danielle Donahue of the Mouse Imaging Facility (MIF), NIH, for preparing and skinning the rat tails. All 14 T MRI experiments were performed at the MIF, NIH.

NMR IN BIOMEDICINE

REFERENCES

1. Henkelman RM, Stanisz GJ, Graham SJ. Magnetization transfer in MRI: a review. NMR Biomed. 2001; 14: 57–64.
2. Tsoref L, Shinar H, Seo Y, Eliav U, Navon G. Proton double-quantum filtered MRI - A new method for imaging ordered tissues. Magn. Reson. Med. 1998; 40: 720–726.
3. Eliav U, Navon G. A study of dipolar interactions and dynamic processes of water molecules in tendon by H-1 and H-2 homonuclear and heteronuclear multiple-quantum-filtered NMR spectroscopy. J. Magn. Reson. 1999; 137: 295–310.
4. Eliav U, Navon G. Multiple quantum filtered NMR studies of the interaction between collagen and water in the tendon. J. Am. Chem. Soc. 2002; 124: 3125–3132.
5. Navon G, Shinar H, Eliav U. Double quantum filtered NMR in ordered biological tissues. *In*: *Encyclopedia of Nuclear Magnetic Resonance*, *Volume* 9. Grant DM, Harris RK *(eds)*. Wiley: Chichester, 2002, p 374–384.
6. Neufeld A, Eliav U, Navon G. New MRI method with contrast based on the macromolecular characteristics of tissues. Magn. Reson. Med. 2003; 50: 229–234.
7. Gatehouse PD, Bydder GM. Magnetic resonance imaging of short T-2 components in tissue. Clin. Radiol. 2003; 58: 1–19.
8. Robson MD, Gatehouse PD, Bydder M, Bydder GM. Magnetic resonance: An introduction to ultrashort TE (UTE) imaging. J. Comput. Assist. Tomogr. 2003; 27: 825–846.
9. Robson MD, Bydder GM. Clinical ultrashort echo time imaging of bone and other connective tissues. NMR Biomed. 2006; 19: 765–780.
10. Du J, Bydder M, Takahashi AM, Chung CB. Two-dimensional ultrashort echo time imaging using a spiral trajectory. Magn. Reson. Imaging 2008; 26: 304–312.
11. Zheng SK, Xia Y. Effect of phosphate electrolyte buffer on the dynamics of water in tendon and cartilage. NMR Biomed. 2009; 22: 158–164.
12. Migchels C, Berendse HJC. Proton exchange and molecular orientation of water in hydrated collagen fibers - Nmr-study of H_2O and D_2O. J. Chem. Phys. 1973; 59: 296–305.
13. Kalk A, Berendsen HJC. Proton magnetic-relaxation and spin diffusion in proteins. J. Magn. Reson. 1976; 24: 343–366.
14. Ernst R, Bodenhausen G, Wokaun *A. Principles of Nuclear Magnetic Resonance in One and Two Dimensions*. Oxford University Press: Oxford, UK, 1987.
15. Saar G, Zilberman Y, Shinar H, Keinan-Adamsky K, Pelled G, Gazit D, Navon G. Monitoring of the effect of intervertebral disc nucleus pulposus ablation by MRI. NMR Biomed. 2010; 23: 554–562.
16. Strocchi R, Leonardi L, Guizzardi S, Marchini M, Ruggeri A. Ultrastructural Aspects of Rat Tail Tendon Sheaths. J. Anat. 1985; 140: 57–67.
17. Grynpas MD, Eyre DR, Kirschner DA. Collagen type II differs from type I in native molecular packing. Biochim. Biophys. Acta 1980; 626: 346–355.
18. Eyre DR, Muir H. Type-1 and type-2 collagens in intervertebral-disk - interchanging radial distributions in annulus fibrosus. Biochem. J. 1976; 157: 267–270.

